ELSEVIER

Colloids and Surfaces B: Biointerfaces 16 (1999) 55–72

COLLOIDS AND SURFACES B

www.elsevier.nl/locate/colsurfb

Solubilization of hydrocarbons and resulting aggregate shape transitions in aqueous solutions of Pluronic® (PEO–PPO–PEO) block copolymers

R. Nagarajan *

Department of Chemical Engineering, The Pennsylvania State University, 161 Fenske Laboratory, University Park, PA 16802, USA

Abstract

Pluronic® block copolymers are commercially available symmetric triblock copolymers with poly(ethylene oxide), PEO, as the hydrophilic end blocks and poly(propylene oxide), PPO, as the hydrophobic middle block. In this paper, the solubilization of hydrocarbons by aggregates of Pluronic® block copolymers in water is examined in the framework of a simple molecular theory of solubilization. The aggregates have an inner core region made up of PPO and the solubilizate and an outer corona region made up of PEO and water. Expressions for the standard state free energy change associated with solubilization of hydrocarbons by aggregates having spherical, cylindrical, and lamellar shapes are presented. These free energy contributions account for the mixing of the core block with the solubilizate, the consequent changes in the state of deformation of the core block, the changes in the state of dilution and deformation of the corona block, the formation of the core-solvent interface, and the backfolding of the triblock copolymer which ensures that the two end blocks are in contact with the solvent. Utilizing these free energy expressions, we predict the core size, the corona thickness, and the aggregation number of the micelle and also the volume fraction of the hydrocarbon solubilized in the core, for seven aromatic and aliphatic hydrocarbon solubilizates incorporated within numerous Pluronic® compounds. The calculated results show that a growth in aggregate size occurs both because of the incorporation of the hydrocarbon and also the increase in the intrinsic number of block copolymer molecules per aggregate. More interestingly, solubilization is shown to induce a transition in aggregate shapes from spheres to cylinders and then to lamellae. The shape transition is found to be critically controlled by the free energy of mixing of the solubilizate with the core forming PPO block.

Keywords: Pluronic® block copolymers; PEO–PPO–PEO triblock copolymers; Block copolymer micelles; Spherical, cylindrical and lamellar aggregates; Solubilization in micelles; Solubilization of hydrocarbons; Thermodynamics of solubilization; Solubilizate-induced aggregate shape transitions

1. Introduction

Block copolymer molecules consisting of hydrophobic and hydrophilic blocks aggregate in aqueous solutions, forming multimolecular aggre-

* Corresponding author.
E-mail address: rxn@psu.edu (R. Nagarajan)

0927-7765/99/$ - see front matter
PII: S0927-7765(99)00061-2

gates having spherical, cylindrical or lamellar morphologies. In these aggregates, the hydrophobic blocks constitute the core and the hydrophilic blocks along with the solvent water form the corona. One of the most useful properties of such aggregates is their ability to incorporate hydrophobic substances, thus enhancing dramatically the effective solubility of these (otherwise) practically insoluble molecules in aqueous solutions. This phenomenon, referred to as solubilization, is made possible by the incorporation of the solubilizates in the hydrophobic microenvironment offered by the aggregate core. Experimental observations as well as theoretical modeling of aggregation and solubilization in block copolymer solutions and also the phase behavior of block copolymer systems have recently been reviewed [1–3]. The phenomenon of solubilization holds promise for many potential applications of aqueous block copolymer solutions such as in chemical extractions, as alternate solvents for separations and serving as reaction media, for environmental remediation, for the separation of biotechnological products and for serving as media for enzymatic biocatalysis.

Experimental results on the solubilization of hydrocarbons in solutions of poly(ethylene oxide)–poly(propylene oxide) (PEO–PPO) and poly(vinyl pyrrolidone)–polystyrene (PVP–PS) block copolymers presented in our previous studies [4] demonstrated large solubilization capacities and high selectivity for aromatics over aliphatics in block copolymer micelles compared to conventional low molecular weight surfactant micelles. To explore the origin of this solubilization behavior, we formulated a simple molecular theory of solubilization in spherical micelles formed of diblock copolymers using a mean-field approach [5] and later extended the model to micelles formed also of symmetric triblock copolymers [6]. In this paper, we apply that thermodynamic theory to predict the solubilization behavior of a widely used class of triblock copolymers that are commercially available under the trade name of Pluronics®, taking into consideration not only the spherical aggregate model but also cylindrical and lamellar aggregates. These symmetric triblock copolymers contain poly(ethylene oxide) as the hydrophilic block (PEO, referred to as the B block) and poly(propylene oxide) as the hydrophobic block (PPO referred to as the A block), with molecular weights ranging between 2500 and 14 600 and the weight fraction of the hydrophilic PEO block between 0.2 and 0.8. The block copolymer is denoted by the symbol $E_xP_yE_x$, where E and P denote the PEO and PPO blocks and x and y are the respective numbers of segments of these blocks. The trade names by which these block copolymers are known such as L64, P85, F127 are also mentioned in the text. In the trade names, the first letter L, P or F refers to the liquid, paste or solid form of the block copolymer, the last digit multiplied by ten gives the mass percent of the PEO block, while the first one or two digits refer to the molecular size of the PPO block. These molecules are widely used because of their commercial availability, and hence the present systematic study is directed towards predicting their behavior in solution.

In the treatment discussed in this paper, we assume uniform segment densities in the core and the corona regions of the aggregates. To maintain such uniform densities, it is necessary for the chains to stretch non-uniformly [7]. Thus, we invoke the terminology, *uniform concentration–non-uniform deformation* model, for describing the present thermodynamic treatment. Micellar models based on such non-uniform chain stretching have been developed and discussed by us earlier for conventional low molecular weight surfactants [8]. Alternate micellar models allowing for radial concentration inhomogeneities in the corona region [8] or in both the core and the corona regions [9] have also been formulated in our previous studies. The former model was based on a mean-field description while the latter theory was based on a scaling approach exploiting the analogy between spherical micelles and star polymers. Another approach to modeling has been described by Hurter et al. [10] involving self-consistent field calculations which allow the prediction of detailed composition profiles in the core and the corona regions of the micelle.

It is pertinent to remark here that the sparse number of available experimental studies of solubilization are limited to providing information on the amount of solubilized species in an aggregate,

often expressed as a molar, mass or volume fraction [4,11–14]. In contrast, a theory of solubilization can predict a priori not only the volume fraction of the solubilizate inside the aggregate core region as a function of the molecular properties of the copolymer, the solvent, and the solubilizate, but also the shape of the equilibrium aggregate and all the microstructural features of the aggregate such as the core radius, the thickness of the corona, and the aggregation number. Such a theory, applicable to both diblock and symmetric triblock copolymer molecules, is outlined below. Predictions of various microstructural features of micelles containing solubilizates are given in this paper for seven aromatic and aliphatic hydrocarbon solubilizates in aggregates formed of 15 Pluronic® triblock copolymers. Wherever possible, comparison is made with the experimental data available in the literature.

2. Theory of solubilization

2.1. Size and composition distribution of aggregates

The aqueous solution is made up of solvent molecules, singly dispersed copolymer and solubilizate molecules and micelles of various sizes and compositions (or equivalently, various aggregation numbers and volume fractions of solubilizates). Each of the species in the solution, including micelles of different sizes and compositions, is treated as a distinct chemical component. The size and composition distribution of micelles at equilibrium is obtained by minimizing the total free energy of the system. In writing the system free energy, the standard state of the solvent is defined as the pure solvent whereas the standard states of all the other components are taken as those at infinitely dilute solution conditions. The standard chemical potentials of the solvent water (W), the singly dispersed copolymer, the singly dispersed solubilizate (J) and micelles of aggregation number g containing j solubilizate molecules, are denoted by μ_W^0, μ_1^0, μ_{1J}^0 and μ_g^0, respectively. (Note that g and j refer to the total numbers of molecules for spherical aggregates, numbers per unit length in the case of cylindrical aggregates and numbers per unit area in the case of lamellae.) Denoting the mole fraction of species i by X_i, the micelle size and composition distribution equation can be written [8,9] in the form

$$X_g = X_1^g X_{1J}^j \exp - \left(\frac{\mu_g^0 - g\mu_1^0 - j\mu_{1J}^0}{kT} \right) \quad (1)$$

In writing Eq. (1), it is assumed that either inter-micelle interactions are not present or that they do not affect the size distribution. Also the system entropy of the multicomponent solution is written as for an ideal solution. In dilute solutions such as those of interest here, the inter-micellar interactions are not important. Therefore, one may neglect the free energy contributions associated with such interactions. The consequences of using a few plausible models of system entropy in the theory of micellization have been analyzed in detail [15]. It was found that for nonionic systems such as those considered here, the choice of a model for the system entropy has no influence on the micellar structural parameters but affects only the magnitude of the critical micelle concentration (CMC). Further, the CMC predicted assuming one entropy model can be related via a simple scale factor to the CMC that would result from another entropy model [15].

If one wants to calculate the saturation amount of solubilization that is possible inside the micelle, then the concentration of the singly dispersed solubilizate X_{1J} in water should be its saturation concentration X_{1J}^*. This condition is defined by the equilibrium relation

$$\mu_J^H = \mu_{1J}^0 + kT \ln X_{1J}^* \quad (2)$$

Since an excess solubilizate phase comes into existence when the aqueous solution is saturated with the solubilizate, the standard state μ_J^H of the solubilizate refers to a pure solubilizate phase. Denoting by f, the fractional saturation of water, with the solubilizate, (i.e. X_{1J}/X_{1J}^*), the micelle size and composition distribution equation becomes

$$X_g = X_1^g f^{j/g} \exp - \left(\frac{g\Delta\mu_g^0}{kT} \right), \text{ where } \Delta\mu_g^0 = \left(\frac{\mu_g^0}{g} - \mu_1^0 - \frac{j}{g}\mu_J^H \right) \quad (3)$$

The factor $\Delta\mu_g^0$ represents the change in the standard state free energy when a singly dispersed block copolymer molecule in water and j/g solubilizate molecules in their pure phase are transferred to an isolated micelle in water. The solubilization limit is achieved for $f=1$, when the aqueous micellar phase coexists with the pure solubilizate phase. All predictions given in this paper are for this condition.

2.2. Pseudophase description of micelles

Our calculations have shown that the size and composition distribution of micelles is typically narrow and it is reasonable to assume for simplicity that the micelles are all of a single size and composition [5]. Therefore, to reduce the numerical computational efforts, the micelle containing the solubilizate can be represented as a pseudophase in equilibrium with the singly dispersed solubilizate and copolymer molecules in solution. For aggregates exhibiting narrow size and composition distribution, this representation provides results practically identical to those obtained from the detailed size distribution calculations. The equilibrium characteristics of the micelle in the pseudophase approximation are obtainable from the condition

$$\frac{\partial}{\partial g}\left[\frac{\Delta\mu_g^0}{kT}\right]=0,\ \frac{\partial}{\partial j}\left[\frac{\Delta\mu_g^0}{kT}\right]=0 \quad \text{at}$$

$$g=g_{\text{opt}},\ j=j_{\text{opt}} \tag{4}$$

where g_{opt} and j_{opt} refer to the numbers of block copolymer and solubilizate molecules, respectively, constituting the optimal or equilibrium aggregate. The critical micelle concentration in the pseudophase approximation is calculated from

$$X_{\text{CMC}}=\exp\left[\frac{\Delta\mu_g^0}{kT}\right] \quad \text{at} \quad g=g_{\text{opt}},\ j=j_{\text{opt}} \tag{5}$$

The magnitude of $\Delta\mu_g^0$controls the CMC as shown by Eq. (5). In contrast, the equilibrium structural features of the micelle are determined by how this standard free energy difference depends on the variables g and j as is evident from Eq. (4). An expression for this free energy difference depends on the geometrical features of the micelle, which are specified below.

2.3. Geometrical properties of aggregates

Two structural descriptions of aggregates can be visualized as shown in Fig. 1, depending upon how the solubilizate is contained inside the block copolymer micelle. These two descriptions result by analogy with the structural models employed for simple solubilization and microemulsification, respectively, in systems involving low molecular weight surfactants. The Type (a) structure is analogous to that used for simple solubilization. Here, the micellar core is made up of the solvent

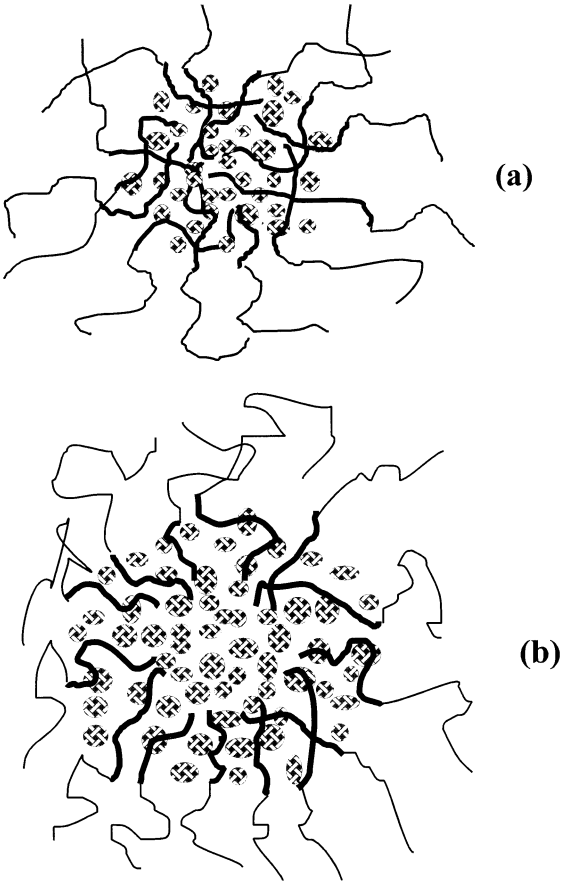

Fig. 1. Schematic representation of a spherical block copolymer micelle containing the solubilizate. The darker lines denote the hydrophobic block and the lighter lines, the hydrophilic block. In Type (a) structure, all of the solubilizate molecules interact with the core block. In Type (b) structure, a part of the solubilizate molecules are present in a separate domain while the remaining interact with the core block.

Table 1
Geometrical properties of spherical, cylindrical and lamellar aggregates

Property[a]	Sphere	Cylinder	Lamella
V_C	$4\pi R^3/3$	πR^2	$2R$
V_S	$V_C[(1+D/R)^3-1]$	$V_C[(1+D/R)^2-1]$	$V_C[(1+D/R)-1]$
g	$V_C\varphi_A/(N_A v_A)$	$V_C\varphi_A/N_A v_A)$	$V_C\varphi_A/(N_A v_A)$
a	$3N_A v_A/(R\varphi_A)$	$2N_A v_A/(R\varphi_A)$	$N_A v_A/(R\varphi_A)$
φ_B	$(N_B v_B)/(N_A v_A)\varphi_A(V_C/V_S)$	$(N_B v_B)/(N_A v_A)\varphi_A(V_C/V_S)$	$(N_B v_B)/(N_A v_A)\varphi_A(V_C/V_S)$
η	$1-\varphi_A$	$1-\varphi_A$	$1-\varphi_A$

[a] Properties refer to: core volume (V_C); corona volume (V_S). Aggregation number of micelle (g); area per molecule of core surface (a); volume fraction of B in corona (φ_B); volume fraction of solubilizate in core (η).

incompatible A blocks and the solubilizate J. The solvent compatible B blocks and solvent W are present in the corona region of the micelle. The Type (b) structure is analogous to that used for droplet microemulsions, with the core region separated into two parts. Pure solubilizate J is allowed to exist in the inner core of the micelle. This solubilizate domain is surrounded by the outer core region consisting of the A block and the solubilizate J. The corona of the micelle contains the B block and the solvent W as in the Type (a) structure. In the absence of a pool of pure solubilizate J in the inner core, the Type (b) structure reduces identically to Type (a). Free energy calculations of the kind described below showed that for many diblock copolymers, the condition of minimum free energy always occurred corresponding to a zero size for the pure solubilizate pool. Thus, the thermodynamic equilibrium criterion always favored the occurrence of the Type (a) structure. Consequently, free energy expressions corresponding to only the Type (a) structure are discussed here. Although Fig. 1 depicts spherical aggregates only, analogous structures can be visualized having cylindrical and lamellar shapes.

The shape of the aggregate and the assumption of incompressibility lead to the geometrical relations summarized in Table 1 for different morphologies [16]. We denote the molecular volumes of the A (PPO) and the B (PEO) segments, the solubilizate and the solvent by v_A, v_B, v_J and v_W, respectively. The characteristic lengths of the A and the B segments are denoted by L_A ($=v_A^{1/3}$) and L_B ($=v_B^{1/3}$). The variables N_A and N_B refer to the number of segments of block A and block B for the AB diblock as well as the BAB triblock copolymers, implying that the BAB triblock copolymer has two terminal blocks of size $N_B/2$ attached to a middle block of size N_A. We use the variable R to denote the hydrophobic core dimension (radius for sphere or cylinder and half bilayer thickness for lamella), D for the corona thickness, and a for the surface area of the aggregate core per constituent block copolymer molecule. The numbers of molecules g and j, the micelle core volume V_C, and the corona volume V_S all refer to the total quantities in the case of spherical aggregates, quantities per unit length in the case of cylindrical aggregates and quantities per unit area in the case of lamellae. The core volume V_C is calculated as the sum of the volumes of the A blocks and the solubilizate molecules, $V_C = gN_A v_A + jv_J$. The volume fraction of the solubilizate molecules in the core is denoted by η ($=jv_J/(gN_A v_A + jv_J)$). The concentrations of segments are assumed to be uniform in the core as well as in the corona, with φ_A standing for the volume fraction of the A segments in the core ($\varphi_A = 1-\eta$), and φ_B for the volume fraction of the B segments in the corona. If any three structural variables are specified all the remaining geometrical variables can be calculated through the relations given in Table 1. For convenience, R, D and η (or φ_A) are chosen as the independent variables.

2.4. Model for the free energy of solubilization

To formulate an expression for the free energy of solubilization $\Delta\mu_g^0$ defined in Eq. (3), we consider all the physicochemical changes accompanying the transfer of the singly dispersed copolymer molecule from the infinitely dilute aqueous solution state and the solubilizate molecule from its pure phase to an isolated micelle in the infinitely dilute solution state. Firstly, the transfer of the solubilizate and the singly dispersed copolymer to the micellar core is associated with changes in the state of dilution and in the state of deformation of the A block, including the swelling of the A blocks inside the core by the solubilizate J. Secondly, the B block of the singly dispersed copolymer is transferred to the corona region of the micelle and this transfer process also involves changes in the states of dilution and deformation of the B block. Thirdly, the formation of the micelle localizes the copolymer such that the A block is confined to the core while the B block is confined to the corona. Fourthly, the formation of the micelle is associated with the generation of an interface between the micelle core made up of A blocks and solubilizate J and the micelle corona consisting of solvent W and B blocks. All these microevents contribute to the free energy of solubilization in the case of both diblock and triblock copolymers. Further, in the case of a BAB triblock copolymer, folding or loop formation of the A block occurs ensuring that the B blocks at the two ends are in the aqueous domain while the folded A block is within the hydrophobic core of the micelle. This provides an additional free energy contribution. The overall free energy of solubilization can be obtained as the sum of the above individual contributions:

$$(\Delta\mu_g^0) = (\Delta\mu_g^0)_{\mathrm{A,\,dil}} + (\Delta\mu_g^0)_{\mathrm{A,\,def}} + (\Delta\mu_g^0)_{\mathrm{B,\,dil}} + (\Delta\mu_g^0)_{\mathrm{B,\,def}} + (\Delta\mu_g^0)_{\mathrm{loc}} + (\Delta\mu_g^0)_{\mathrm{int}} + (\Delta\mu_g^0)_{\mathrm{loop}} \quad (6)$$

Expressions for each of these contributions are formulated below.

2.5. Change in state of dilution of block A

In the singly dispersed state of the copolymer molecule in water, the A block is in a collapsed state minimizing its interactions with the solvent. We consider the region consisting of the collapsed A block with some solvent entrapped in it to be a spherical globule, whose diameter $2R_{\infty\mathrm{A}}$ is equal to the end-to-end distance of block A in the solvent. The volume of this spherical region is denoted by $V_{\infty\mathrm{A}}$. The chain expansion parameter α_{A} describes the swelling of the polymer block A by the solvent W.

$$V_{\infty\mathrm{A}} = \frac{4\pi R_{\infty\mathrm{A}}^3}{3},\ 2R_{\infty\mathrm{A}} = \alpha_{\mathrm{A}} N_{\mathrm{A}}^{1/2} L_{\mathrm{A}},\ \alpha_{\mathrm{A}} = \left(\frac{6}{\pi}\right)^{1/3} N_{\mathrm{A}}^{-1/6} \varphi_{\mathrm{A1}}^{-1/3} \quad (7)$$

where φ_{A1} ($= N_{\mathrm{A}} v_{\mathrm{A}} / V_{\infty\mathrm{A}}$) is the volume fraction of A segments within the monomolecular glo-bule. The first equality in Eq. (7) follows from geometry, while the second equality is based on the definition of the chain expansion parameter α_{A}, taking ($N_{\mathrm{A}}^{1/2} L_{\mathrm{A}}$) as the unperturbed end-to-end distance of block A. The third equality is obtained by combining the first two in conjunction with the definition for φ_{A1}. The volume fraction φ_{A1} is calculated as suggested by de Gennes [17], from the condition of osmotic equilibrium between the monomolecular globule treated as a distinct phase and the solvent surrounding it.

$$\ln(1-\varphi_{\mathrm{A1}}) + \varphi_{\mathrm{A1}} + \chi_{\mathrm{AW}} \varphi_{\mathrm{A1}}^2 = 0 \quad (8)$$

In Eq. (8), χ_{AW} is the Flory interaction parameter between the pure A polymer and water. In the micelle, the A block is confined to the core region where it is swollen by the solubilizate J. We consider this region to be uniform in concentration with a volume fraction φ_{A} of A segments and η ($= 1 - \varphi_{\mathrm{A}}$) of the solubilizate. A mean-field description is employed for calculating the free energy of this region. The difference in the dilution of block A from its singly dispersed state to the micellized state makes a free energy contribution given by the relation

$$\frac{(\Delta\mu_g^0)_{A,\,dil}}{kT} = N_A\left[\frac{v_A}{v_J}\frac{1-\varphi_A}{\varphi_A}\ln(1-\varphi_A) + \frac{v_A}{v_J}(1-\varphi_A)\chi_{AJ}\right]$$
$$- N_A\left[\frac{v_A}{v_J}\frac{1-\varphi_{A1}}{\varphi_{A1}}\ln(1-\varphi_{A1}) + \frac{v_A}{v_W}(1-\varphi_{A1})\chi_{AW} + \left(\frac{\sigma_{AW}L_A^2}{kT}\right)\frac{6}{\alpha_A N_A^{1/2}}\right] \quad (9)$$

In this equation, the first two terms account for the entropic and enthalpic contributions arising from the mixing of pure A block and the pure solubilizate J within the micellar core. They are written in the form of the Flory expression for the swelling of a network [18] by a solvent. The third and the fourth terms account for the entropic and enthalpic changes associated with the removal of A block from its infinitely dilute state in water to a pure A state. These terms are written in the framework of the Flory expression [18] for an isolated polymer molecule. The last term accounts for the fact that the interface of the globule of the singly dispersed A block disappears on micellization. This term is written as the product of the interfacial tension (σ_{AW}) between pure A and solvent W, the surface area of the globule ($4\pi R_{\infty A}^2$) and the factor φ_{A1} (volume fraction of the polymer A in the globule) to account for the reduction in the contact area between the block A and solvent W caused by the presence of some water molecules inside the monomolecular globule. If the interfacial tension σ_{AW} is not available from direct measurements, it can be estimated using the relation $\sigma_{AW} = (\chi_{AW}/6)^{1/2}(kT/L^2)$, where $L = v_W^{1/3}$. Such a relation is usually employed for the calculation of polymer–polymer interfacial tensions.

2.6. Change in state of deformation of block A

In the singly dispersed state of the copolymer, the conformation of the A block is characterized by the chain expansion parameter α_A which is the ratio between the actual end-to-end distance and the unperturbed end-to-end distance of the polymer block. The free energy of this deformation is written using the Flory expression [18] derived for an isolated polymer molecule. Within the micelle, the A block is stretched non-uniformly, with the chain ends occupying a distribution of positions within the core while ensuring that the core has an uniform concentration. The free energy contribution allowing for non-uniform chain deformation is calculated using the analysis of chain packing pioneered by Semenov [7]. In the case of a BAB triblock copolymer, the A block deformation is calculated by considering the folded A block of size N_A to be equivalent to two A blocks of size $N_A/2$. On this basis, one obtains

$$\frac{(\Delta\mu_g^0)_{A,\,def}}{kT} = \left[q\left(\frac{p\pi}{80}\right)\frac{R^2}{(N_A/q)L_A^2}\right] - \left[\frac{3}{2}(\alpha_A^2 - 1) - \ln\alpha_A^3\right] \quad (10)$$

where $q = 1$ for a AB diblock copolymer and $q = 2$ for a BAB triblock copolymer having a middle hydrophobic block. The parameter p is dependent on aggregate shape and has the value of 3 for spherical micelles, 5 for cylinders and 10 for lamellae [7,8]. In Eq. (10), the first term represents the A block deformation free energy in the micelle while the second term corresponds to the deformation free energy in the singly dispersed copolymer.

2.7. Change in state of dilution of block B

In the singly dispersed state of the copolymer, the polymer block B is swollen with the solvent. As mentioned before, N_B denotes the size of the B block for the AB diblock copolymer while for a symmetric BAB triblock copolymer, the end blocks are of equal size $N_B/2$. We consider this swollen B block to be a sphere, whose diameter $2R_{\infty B}$ is equal to the end-to-end distance of isolated block B in the solvent. The volume of this spherical region is denoted by $V_{\infty B}$ while φ_{B1} ($= N_B v_B/V_{\infty B}$) is the volume fraction of B segments within the monomolecular globule.

$$V_{\infty B} = \frac{4\pi R_{\infty B}^3}{3},\ 2R_{\infty B} = \alpha_B(N_B/q)^{1/2}L_B \quad (11)$$

The second equality in Eq. (11) is based on the definition of the chain expansion parameter α_B, which can be estimated using the expression developed by Flory [18]. In the Flory expression for α_B, Stockmayer [19] has suggested decreasing the numerical coefficient by approximately a factor of two to ensure consistency with the results obtained from perturbation theories of excluded volume. Consequently, one can estimate α_B as the solution of

$$\alpha_B^5 - \alpha_B^3 = 0.88(1/2 - \chi_{BW})(N_B/q)^{1/2} \quad (12)$$

where χ_{BW} is the Flory interaction parameter between the B block and water.

In the micelle, the B blocks are present in the corona region of volume V_S. This region is assumed to be uniform in concentration with φ_B ($= gN_Bv_B/V_S$) being the volume fraction of the B segments in the corona. The free energy of the corona region can be written using the Flory expression (Eq. (14)) for a network swollen by the solvent. Therefore, the difference in the states of dilution of the B block on micellization provides the following free energy contribution:

$$\frac{(\Delta\mu_g^0)_{B,\,dil}}{kT} = N_B\left[\frac{v_B}{v_W}\frac{1-\varphi_B}{\varphi_B}\ln(1-\varphi_B) + \frac{v_B}{v_W}(1-\varphi_B)\chi_{BW}\right] - N_B\left[\frac{v_B}{v_W}\frac{1-\varphi_{B1}}{\varphi_{B1}}\ln(1-\varphi_{B1}) + \frac{v_B}{v_W}(1-\varphi_{B1})\chi_{BW}\right] \quad (13)$$

The first two terms in Eq. (13) describe the entropic and enthalpic contributions to the free energy of swelling of the B block by the solvent in the corona region of the micelle while the last two terms refer to the corresponding contributions in the singly dispersed copolymer molecule.

2.8. Change in state of deformation of block B

In the singly dispersed state, the B block has a chain conformation characterized by the chain expansion parameter α_B. In the micelle, the B block is stretched non-uniformly over the micelle corona so as to ensure that the concentration in the corona region is uniform. Semenov [7] has shown that the estimate for the chain deformation energy assuming that the termini of all B blocks lie at the distance D from the core surface is not very different from that calculated assuming a distribution of chain termini at various positions within the corona. On this basis, one can write [6,16]

$$\frac{(\Delta\mu_g^0)_{B,\,def}}{kT} = \left[q\frac{3}{2}\frac{L_BR}{(a/q)\varphi_B}P\right] - q\left[\frac{3}{2}(\alpha_B^2 - 1) - \ln\alpha_B^3\right] \quad (14)$$

where a is the surface area per molecule of the micelle core, $q = 1$ for AB diblock and 2 for BAB triblock, as mentioned before, and P is a shape-dependent function given by $P = (D/R)/[1 + (D/R)]$ for spheres, $P = \ln[1 + (D/R)]$ for cylinders and $P = (D/R)$ for lamellae [6,16]. The first term in Eq. (14) represents the free energy of deformation of the B block in the micellar corona while the second term denotes the corresponding free energy in the singly dispersed copolymer molecule.

2.9. Localization of the copolymer molecule

On micellization, the copolymer becomes localized in the sense that the joint linking blocks A and B in the copolymer is constrained to remain in the interfacial region rather than occupying all the positions available in the entire volume of the micelle. The entropic reduction associated with localization is modelled using the concept of configurational volume restriction. Thus, the localization free energy is calculated on the basis of the ratio between the volume available to the A–B joint in the interfacial shell of the micelle (surrounding the core and having a thickness L_B) and the total volume of the micelle.

$$\frac{(\Delta\mu_g^0)_{loc}}{kT} = -q\ln\left[\frac{dL_B}{R(1 + D/R)^d}\right] \quad (15)$$

Here, d refers to the dimensionality of aggregate growth and is 3 for spherical micelles, 2 for cylinders and 1 for lamellae [6,16].

2.10. Formation of micellar core-solvent interface

When micelle forms, an interface is generated between the core region consisting of the A block and the solubilizate J and the corona region con-

sisting of the B block and the solvent W. The free energy of formation of this interface is estimated as the product of the surface area of the micellar core and an interfacial tension characteristic of this interface. The appropriate interfacial tension is that between a solution of block A and solubilizate J in the micelle core and a solution of block B and solvent W in the micellar corona. Since the corona region is often very dilute in block B, the interfacial tension can be approximated as that between the solvent W and a solution of the A block and the solubilizate J in the micelle core. Denoting the polymer A–solvent W interfacial tension by σ_{AW} and the solubilizate J–solvent W interfacial tension by σ_{JW}, the free energy of generation of the micellar core–solvent interface is calculated from

$$\frac{(\Delta\mu_g^0)_{int}}{kT} = \frac{\sigma_{agg}}{kT}a,\ \sigma_{agg} = \sigma_{AW}\varphi_A + \sigma_{JW}(1-\varphi_A) \tag{16}$$

Here, the interfacial tension of a polymer solution of block A and solubilizate J against another liquid W is approximated to be the composition-averaged interfacial tensions of pure polymer A and pure solubilizate J against the solvent W. The volume fraction is used as the composition variable. Such a simple dependence of the interfacial tension on bulk solution composition is not generally obeyed in case of free solutions of polymers or of low molecular weight components. The origin of the deviation from linearity lies in the preferential adsorption or depletion of one of the components at the interface, which causes the surface composition to differ from the bulk composition [20]. However, the micellar interface is different from the interface of a free polymer solution. Specifically, because of the localization of the A–B link at the interface, the segments of the A blocks are forced to be at the interface independent of any selective adsorption or depletion. This would diminish somewhat the difference between the surface and bulk compositions in the micellar core when compared to that in a free polymer solution. Consequently, the composition-averaging of interfacial tension expressed by Eq. (16) is taken as a reasonable approximation in the present calculations. An alternate approach to estimating the interfacial tension by calculating the interface composition between two bulk solutions has been explored in our study of solubilization in low molecular weight surfactant micelles [8].

2.11. Backfolding or looping in triblock copolymer

The backfolding or looping of the middle block in a BAB triblock copolymer contributes an entropic term to the free energy of solubilization. This contribution is absent for a diblock copolymer. Jacobson and Stockmayer [21] showed that the reduction in entropy for the condition that the ends of a linear chain of N segments are to lie in the same plane or on one side of a plane is proportional to $\ln N$. Therefore, the assumption that the backfolding of the middle block in the micelle follows the same functional form is made. Hence, the backfolding makes the following contribution for a BAB copolymer.

$$\frac{(\Delta\mu_g^0)_{loop}}{kT} = \frac{3}{2}\beta\ \ln[N_A] \tag{17}$$

Here, β is an excluded volume parameter which is equal to unity when the excluded volume effects are negligible and larger than unity when these effects become important. In our calculations, β is taken to be unity [6,16].

3. Model predictions and discussion

3.1. Estimation of molecular constants

To carry out quantitative calculations, the values of molecular constants appearing in Eqs. (7)–(17) are needed for the PEO–PPO–PEO triblock copolymers, solvent water and hydrocarbon solubilizates. The molecular volumes of the segments are $v_A = 96.5$ Å^3 (for PO) and $v_B = 64.6$ Å^3 (for EO) while for water, $v_W = 30$ Å^3. Knowing that the molecular weights of the segments are 58 for PO and 44 for EO, the number of PEO and PPO segments are calculated for various Pluronic® block copolymers. The molecular volumes v_J of the solubilizates, the Hildebrand-Scatchard solu-

bility parameters δ_J, and the interfacial tensions σ_{JW} between water and the solubilizates are listed in Table 2. The Flory interaction parameter χ_{AJ} accounts for the interactions between the core forming block A of the copolymer and the solubilizate J. This parameter is estimated [4] from knowledge of the Hildebrand solubility parameters of both A and J via the relation $\chi_{AJ} = (\delta_A - \delta_J)^2 v_J/kT$, where δ_A is the solubility parameter for the A block, k is the Boltzmann constant and T the absolute temperature. Taking $\delta_A = 19$ MPa$^{1/2}$ for PPO [4] and using the molecular properties of solubilizates listed in Table 2, one can calculate χ_{AJ} for all the solubilizates. The Flory interaction parameters χ_{AW} and χ_{BW} have been estimated to be 2.1 and 0.1, respectively, based on available vapor–liquid equilibrium data on aqueous solutions of PEO and PPO [8]. (The computed results [6] are based on $\chi_{BW} = 0.1$ and not 0.2 as indicated in the text of that reference). It is useful to note that, in reality, the Flory model is not capable of quantitatively describing the observed vapor–liquid and liquid–liquid phase behavior of PEO–water and PPO–water systems. Indeed, it has been found necessary to postulate interaction parameters that are dependent on the temperature, solution composition and the polymer molecular weight in order to achieve quantitative accuracy in the correlation of solution thermodynamic properties [22]. Further, the interaction parameter, with its dependence on the temperature, composition and molecular weight chosen to describe the liquid–liquid phase equilibrium behavior, is not able to describe the vapor–liquid equilibrium data and entirely new dependencies for the interaction parameter have to be created for correlating each type of equilibrium data [22]. This fact should be kept in mind while comparing the theoretical predictions of micellization and solubilization in the Pluronic® block copolymers with experimental data.

Table 2
Molecular properties of the hydrocarbon solubilizates

Solubilizate	v_J (Å^3)	σ_{JW} (dyne cm^{-1})	δ_J (MPa$^{1/2}$)
Benzene	146	33.93	18.80
Toluene	176	36.1	18.19
O-Xylene	200	36.1	18.40
Ethyl benzene	204	38.4	17.99
Cyclohexane	179	50.2	16.76
Hexane	217	50.7	14.92
Heptane	243	51.2	15.13
Octane	270	51.5	15.53
Decane	323	52.0	15.74

3.2. Predicting the formation of solubilizate-free aggregates

The aggregation properties of the block copolymers in the absence of solubilizate have been first computed and the results are summarized in Table 3. In performing these calculations, η appearing in various free energy expressions is set equal to 0; the solubilizate-related free energy terms are not relevant and the free energy minimization is done with respect to the two independent variables R and D. The aggregate shape that yields the smallest free energy of aggregation is taken to be the equilibrium shape. The equilibrium aggregate morpholgy is denoted in the Tables by the symbols L, C, and S, which refer to lamellar, cylindrical and spherical aggregates. Also given are the dimensions of the core region (R) and the corona region (D), and the aggregation number (g) in the case of spherical aggregates. The numerical values within brackets provided in the Table are some available experimental data. The calculations show that the lamellar aggregates are favored when the ratio of PEO:PPO is small whereas spherical aggregates are favored when the PEO:PPO ratio is large. Typically, for block copolymers containing 40 or more weight percent PEO, only spherical aggregates form at 25°C. For block copolymers containing 30 wt% PEO, cylindrical aggregates are possible. Block copolymers containing 20 or less weight percent PEO generate lamellae. One may note that if the temperature is increased, the PEO–water interaction parameter χ_{BW} would increase. In the framework of the free energy model, this increase would lead to a shifting of the shape transitions to higher PEO weight percents. For example, the P85 block copolymer which forms spherical aggregates at 25°C will generate cylindrical aggregates at higher temperatures (corre-

Table 3
Core size R (Å), corona thickness D (Å), shape and/or aggregation number g of solubilizate-free micelles

Trade name	Structure	R (Å)	D (Å)	g for spheres	Shape
L62	$E_6P_{35}E_6$	7.5	19.2		L
L63	$E_9P_{32}E_9$	14.5	13.9		L
L64	$E_{13}P_{30}E_{13}$	34.1 (38–46[a])	16.6 (37–44[a])	57 (39–70[a])	S
P65	$E_{19}P_{29}E_{19}$	30.7	22.1	43	S
F68	$E_{77}P_{29}E_{77}$	21.3 (25[b])	51.0 (53[b])	15 (22[b])	S
P84	$E_{19}P_{43}E_{19}$	42.2	22.5	75	S
P85	$E_{26}P_{40}E_{26}$	36.3 (37[c])	28.3 (36[c])	53 (57[c], 37–78[d])	S
F88	$E_{104}P_{39}E_{104}$	25.0	63.9	17	S
F98	$E_{118}P_{45}E_{118}$	26.7	70.3	18	S
P103	$E_{17}P_{60}E_{17}$	38.6	21.5		C
P104	$E_{27}P_{61}E_{27}$	51.0	29.8	94	S
P105	$E_{37}P_{56}E_{37}$	43.9	37.3	65	S
F108	$E_{133}P_{50}E_{133}$	28.3 (25.0[c])	76.6 (150[c])	20 (13[c])	S
P123	$E_{20}P_{70}E_{20}$	42.1	24.4		C
F127	$E_{100}P_{64}E_{100}$	37.5	70.2	35 (15–45[e], 30[f])	S

[a] 8–32 wt% polymer and between 23 and 35°C using SANS [13].
[b] From Ref. [27] as interpreted and reported in Ref. [11].
[c] Based on light scattering and ultracentrifugation at 37°C [11].
[d] Measurements using SANS in the range 20–40°C [24].
[e] In the range 30–40°C [25].
[f] At 25°C [26].

sponding to a larger value for χ_{BW}), as has been observed experimentally [23,24].

3.3. Prediction of solubilization capacity

The predicted volume fraction of solubilized hydrocarbon in aggregate core are summarized in Table 4 for seven hydrocarbons and 15 Pluronic® block copolymers. The aggregate shape is indicated as before by the symbols L, C and S. Also shown within parenthesis are experimentally measured solubilization capacities available in the literature (also expressed as volume fractions in the micelle core). In general, the agreement between the experimental and measured values of η is reasonably satisfactory. We do observe that for F127, the experimental values, determined in our earlier studies [4], are consistently larger than the predicted values. We discuss at the end, various factors that may be responsible for such a disagreement. In general, the calculated results show that whenever lamellar aggregates are formed, the solubilization capacity of the aggregates is the largest. The solubilization capacity progressively diminishes as we move from lamellar to cylindrical and then to spherical aggregates. The predicted results show that the solubilization capacity is larger when the core block A–solubilizate J interactions are favorable (small χ_{AJ}), the solubilizate–solvent interfacial tension (σ_{JW}) is lower and the molecular volume of the solubilizate (v_J) is smaller. Consequently, the aromatic molecules are found to display a larger solubilization limit compared to the aliphatic molecules.

3.4. Solubilizate-induced aggregate shape transitions

More detailed microstructural information, namely the core dimension R and the corona thickness D, predicted for the various equilibrium aggregates containing solubilizates are summarized in Table 5. Solubilization is found to increase the micellar core radius; the larger the solubilization capacity, the more significant are the changes in R. However, the increase in the core radius R results not only from the incorporation of the solubilizate but also because of the

increasing number of block copolymer molecules that are accommodated within a micelle. This increase in g is significant in the case of solubilizates whose uptake by the micelles is large (see for example P65, P85, P105 and F127, where spherical aggregates are present for all the solubilizates investigated, and therefore the influence of solubilization on aggregate structure can be compared in the absence of a shape change). In comparison, the corona thickness D is not very much affected by solubilization. The core dimension is very strongly influenced by the equilibrium shape of the aggregate. In general, the core dimension R decreases appreciably, whereas the corona thickness D only marginally increases, when the aggregate morphology changes from sphere to cylinder to lamellae.

To understand the origin of the solubilizate-induced transition in aggregate shapes, one can look at the various free energy contributions. In Table 6, for illustrative purposes, the free energy contributions to micellization (the case of no solubilizate) and solubilization in the spherical, cylindrical and lamellar aggregates are compared for P84 block copolymer. Also shown are the aggregate dimensions R and D that yield the lowest free energies for a given aggregate shape. The first entry in each sub-section of the table gives the results predicted for the spherical aggregates. Here all the free energy contributions are the calculated values corresponding to the spherical aggregate. In general, the contribution from the dilution of A block including the swelling of the core by the solubilizate (A, Dil) is negative

Table 4
Volume fraction of solubilized hydrocarbon in micelle core and aggregate morphology[a]

Trade Name	Structure	Benzene	Toluene	Xylene	Ethyl Benzene	Cyclo hexane	Hexane	Decane
L62	$E_6P_{35}E_6$	0.384 (L)	0.315 (L) (0.34)[b]	0.287 (L)	0.256 (L)	0.179 (L)	0.064 (L)	0.033 (L)
L63	$E_9P_{32}E_9$	0.398 (L)	0.327 (L)	0.297 (L)	0.263 (L)	0.172 (L)	0.059 (L)	0.028 (L)
L64	$E_{13}P_{30}E_{13}$	0.414 (L)	0.236 (C) (0.403)[b]	0.207 (C) (0.39)[c]	0.177 (C)	0.107 (C)	0.029 (C)	0.011 (S)
P65	$E_{19}P_{29}E_{19}$	0.268 (S)	0.195 (S) (0.46)[b]	0.167 (S)	0.139 (S)	0.08 (S)	0.025 (S)	0.009 (S)
F68	$E_{77}P_{29}E_{77}$	0.203 (S)	0.13 (S)	0.105 (S)	0.081 (S)	0.038 (S)	0.011 (S)	0.003 (S)
P84	$E_{19}P_{43}E_{19}$	0.481 (L)	0.301 (C) (0.40)[b]	0.271 (C)	0.237 (C)	0.153 (C)	0.045 (S)	0.02 (S)
P85	$E_{26}P_{40}E_{26}$	0.32 (S)	0.243 (S)	0.213 (S)	0.182 (S)	0.11 (S)	0.036 (S)	0.014 (S)
F88	$E_{104}P_{39}E_{104}$	0.248 (S)	0.167 (S)	0.139 (S)	0.111 (S)	0.056 (S)	0.016 (S)	0.004 (S)
F98	$E_{118}P_{45}E_{118}$	0.268 (S)	0.185 (S)	0.155 (S)	0.125 (S)	0.065 (S)	0.019 (S)	0.006 (S)
P103	$E_{17}P_{60}E_{17}$	0.507 (L) (0.441)	0.442 (L) (0.375)[b]	0.415 (L) (0.305)[b]	0.382 (L)	0.278 (L)	0.074 (C)	0.04 (C)
P104	$E_{27}P_{61}E_{27}$	0.538 (L)	0.362 (C) (0.374)[b](C)	0.331 (C)	0.296 (C)	0.177 (S)	0.061 (S)	0.031 (S)
P105	$E_{37}P_{56}E_{37}$	0.379 (S)	0.301 (S)	0.269 (S)	0.235 (S)	0.151 (S)	0.05 (S)	0.023 (S)
F108	$E_{133}P_{50}E_{133}$	0.286 (S)	0.201 (S)	0.169 (S)	0.138 (S)	0.074 (S)	0.022 (S)	0.007 (S)
P123	$E_{20}P_{70}E_{20}$	0.531 (L)	0.468 (L) (0.382)[b]	0.442 (L)	0.41 (L)	0.305 (L)	0.083 (C)	0.048 (C)
F127	$E_{100}P_{64}E_{100}$	0.366 (S) (0.51)[d]	0.279 (S) (0.40)[d]	0.245 (S) (0.33)[d]	0.208 (S) (0.41)[d]	0.124 (S) (0.18)[d]	0.039 (S) (0.08)[d]	0.016 (S) (0.06)[c]

[a] L, lamella; C, cylinder; S, sphere.
[b] Measurements at 5 wt% polymer at 25°C using head space gas chromatography [12].
[c] Measurements at 8–32 wt% polymer and in the range of 23–35°C using SANS [13].
[d] Measurements at 10 wt% polymer at 25°C using gas chromatography [4].

Table 5
Core size R (Å), corona thickness D (Å), shape and/or aggregation number g of micelles containing solubilized hydrocarbons

Trade Name	Structure	Benzene	Toluene	Xylene	Ethyl Benzene	Cyclo hexane	Hexane	Decane
L62	$E_6P_{35}E_6$	24.6, 8.7 L	23.3, 8.88 L	22.6, 8.92 L	22.2, 9.0 L	21.3, 9.23 L	18.8, 9.22 L	18.1, 9.21 L
L63	$E_9P_{32}E_9$	21.8, 13.4 L	20.3, 13.7 L	19.7, 13.7 L	19.1, 13.8 L	17.9, 14.1 L	15.6, 14.0 L	15.0, 14.0 L
L64	$E_{13}P_{30}E_{13}$	19.3, 18.9 L	29.2, 17.6 C	28.4, 17.6 C	27.7, 17.6 C	26.4, 17.8 C	35.2, 16.7 S 61	34.5, 16.6 S 59
P65	$E_{19}P_{29}E_{19}$	39.1, 22.5 S 65	36.7, 22.6 S 59	35.8, 22.5 S 56	35.0, 22.5 S 55	33.6, 22.6 S 52	31.6, 22.3 S 46	31.0, 22.2 S 44
F68	$E_{77}P_{29}E_{77}$	26.0, 54.4 S 21	24.3, 53.3 S 19	23.7, 52.9 S 18	23.2, 52.6 S 17	22.4, 52.0 S 16	21.6, 51.3 S 15	21.4, 51.1 S 15
P84	$E_{19}P_{43}E_{19}$	26.1, 25.6 L	38.7, 23.9 C	37.5, 23.9 C	36.5, 24.1 C	34.5, 24.4 C	44.3, 22.7 S 83	43.1, 22.6 S 79
P85	$E_{26}P_{40}E_{26}$	49.1, 29.0 S 88	45.8, 29.0 S 80	44.4, 29.0 S 75	43.3, 29.0 S 73	41.3, 29.1 S 68	37.9, 28.5 S 57	37.0, 28.4 S 54
F88	$E_{104}P_{39}E_{104}$	32.0, 69.2 S 27	29.6, 67.7 S 24	28.7, 67.0 S 22	28.0, 66.6 S 21	26.8, 65.7 S 20	25.5, 64.4 S 18	25.1, 64.1 S 17
F98	$E_{118}P_{45}E_{118}$	35.1, 76.8 S 31	32.3, 75.0 S 26	31.2, 74.2 S 25	30.4, 73.7 S 24	29.0, 72.7 S 22	27.4, 71.1 S 19	26.9, 70.6 S 19
P103	$E_{17}P_{60}E_{17}$	36.2, 22.3 L	33.7, 22.7 L	32.6, 22.8 L	31.7, 23.1 L	29.3, 23.8 L	42.0, 21.7 C	40.5, 21.7 C
P104	$E_{27}P_{61}E_{27}$	34.5, 33.6 L	50.4, 31.7 C	48.6, 31.7 C	47.3, 31.9 C	62.3, 30.7 S 142	54.7, 30.2 S 109	52.9, 30.0 S 102
P105	$E_{37}P_{56}E_{37}$	63.8, 38.6 S 125	59.1, 38.7 S 112	57.2, 38.6 S 106	55.6, 38.6 S 102	52.5, 38.8 S 95	46.6, 37.8 S 74	45.1, 37.5 S 69
F108	$E_{133}P_{50}E_{133}$	38.1, 84.2 S 34	34.9, 82.2 S 29	33.7, 81.3 S 27	32.8, 80.6 S 26	31.1, 79.5 S 24	29.1, 77.4 S 21	28.6, 76.8 S 20
P123	$E_{20}P_{70}E_{20}$	40.9, 25.1 L	38.1, 25.7 L	36.8, 25.8 L	35.8, 26.1 L	33.1, 27.0 L	46.3, 24.7 C	44.5, 24.6 C
F127	$E_{100}P_{64}E_{100}$	55.2, 77.1 S 72	50.2, 75.7 S 61	48.3, 75.0 S 57	46.7, 74.5 S 54	43.7, 73.7 S 49	39.3, 71.0 S 39	38.2, 70.3 S 37

and is responsible for the occurrence of solubilization. All other free energy contributions are positive. Of these, the contributions associated with the stretching of the core block (A, Def), the stretching of the corona block (B, Def) and the mixing of the corona region (B, Dil) and the formation of the micellar core-shell interface (int) are the important positive free energy contributions that influence all the structural characteristics of micelles. In contrast, the free energy of localization (loc) has only a weak dependence on the aggregation number and on the nature of the solubilizate; thus it has negligible effect on the microstructural parameters. Similarly, the free energy contribution associated with looping of the A block in the triblock copolymer (loop) is a constant and has no influence on the structural parameters.

One can consider the various contributions with respect to aggregate shape by first reviewing the results for micellization in the absence of any solubilizate. The second entry in each sub-section of the table provides the difference between the free energy contributions between a cylinder and a sphere, a negative value representing a contribution favoring the cylinder over the sphere. Similarly, the third entry provides the difference in the free energy contributions between a lamalla and a sphere with a negative entry indicating a preference for lamellar aggregates. We note that the free energy contributions associated with A block deformation (A, Def) and formation of interface

(int) provide negative energy differences indicating that these terms favor non-spherical aggregates. The decrease in the A block deformation contribution arises because of the smaller core dimension consistent with cylindrical and lamellar geometries. The decrease in the interfacial free energy arises from the smaller area per molecule consistent with the non-spherical geometries. These negative free energy differences are, however, overcompensated by the positive free energy differences associate with the corona block deformation (B, Def) and mixing (B, Dil) terms. The corona block dimensions are not significantly altered by a change in the aggregate shape. Therefore, the concentration of the polymer segments in the corona region increases when the sphere changes to a cylinder or a lamella leading to a larger free energy of mixing (B, Dil) contribution for the corona. Similarly, the stretching of the corona block keeping the concentration in the corona region uniform costs a larger free energy (B, Def) for the lamellar and cylindrical aggregates compared to spheres. Since the overall differences in the free energy is positive for cylinders and lamella (see column marked Total $\Delta\mu_g^0$), spherical aggregates are favored in the solubilizate-free sytem. When the solubilizate is added, the above general features remain unaltered but there is an additional negative free energy difference due to the mixing of the solubilizate with the core block (A, Dil). The lower free energy of A block-solubilizate mixing in lamellae with respect to cylinder, and for cylinder compared to sphere, arises from the increasing volume fraction of the solubilizate as the aggregate shape changes from sphere to cylinder to lamella. This negative free

Table 6
Difference in standard free energies per molecule (in units of kT) between non-spherical and spherical aggregates for the solubilization of hydrocarbons in P 84 block copolymer

Aggregate	Contributions to $(\Delta\mu_g^0)$					Total $(\Delta\mu_g^0)$	η	R (Å)	D (Å)
	A, def.	A, dil.	Int.	B, def.	B, dil.				
No solubilizate									
Sphere[a]	2.52	−67.95	18.28	4.76	1.09	−30.57	0	42.2	22.5
Cyl-Sph[b]	−0.65	0	−0.42	0.43	1.07	0.33	0	28.8	23.8
Lam-Sph[c]	−1.74	0	−0.62	1.42	4.32	2.95	0	14.5	26.2
Solubilizate-hexane									
Sphere	2.82	−69.99	19.03	4.83	1.20	−31.36	0.045	44.3	22.7
Cyl-Sph	−0.66	−0.19	−0.40	0.46	1.10	0.22	0.051	30.6	24.0
Lam-Sph	−1.79	−0.68	−0.55	1.51	4.41	2.54	0.072	16.1	26.5
Solubilizate-cyclohexane									
Sphere	3.49	−74.48	20.59	4.94	1.39	−33.28	0.132	48.7	23.0
Cyl-Sph	−0.65	−0.62	−0.32	0.49	1.14	−0.03	0.153	34.5	24.4
Lam-Sph	−1.74	−2.38	−0.25	1.62	4.47	1.52	0.221	19.8	26.9
Solubilizate-toluene									
Sphere	4.28	−79.16	21.8	4.75	1.24	−36.32	0.265	53.6	22.7
Cyl-Sph	−0.59	−0.9	−0.34	0.43	1.05	−0.41	0.301	38.7	23.9
Lam-Sph	−1.54	−3.17	−0.41	1.34	3.86	−0.09	0.41	24.0	26.0
Solubilizate-benzene									
Sphere	4.90	−83.83	22.81	4.64	1.15	−39.57	0.338	57.0	22.5
Cyl-Sph	−0.61	−1.02	−0.41	0.40	0.99	−0.66	0.376	41.5	23.6
Lam-Sph	−1.58	−3.57	−0.7	1.24	3.59	−1.03	0.481	26.1	25.6

[a] Contribution refers to spherical aggregates $(\Delta\mu^0)_{Sph}$.
[b] Each entry represents the difference $(\Delta\mu^0)_{Cyl}-(\Delta\mu^0)_{Sph}$.
[c] Each entry represents the difference $(\Delta\mu^0)_{Lam}-(\Delta\mu^0)_{Sph}$.

energy difference is small when hexane is the solubilizate (consistent with a larger value for χ_{AJ}). Therefore, the total free energy difference remains positive for cylinders (0.22) and lamellae (2.54) suggesting that the spherical aggregates continue to be the equilibrium structures. When the solubilizate is cyclohexane, the difference in the total free energy term becomes negative for cylinders (-0.03) while remaining positive for lamellae (1.52) indicating the favorable formation of cylindrical aggregates. When the solubilizate is toluene, the difference in the total free energy term is negative both for cylindrical (-0.41) and lamellar (-0.09) aggregates. However, the magnitude of the term for cylinder is larger (implying a lower total free energy), thus cylindrical aggregates are favored. When benzene is solubilized, as before, the difference in the total free energy term is negative both for cylindrical (-0.66) and lamellar (-1.03) aggregates. In this case, the magnitude of the term for a lamella is larger than that for the cylinder and hence, lamellar aggregates are favored. One can observe that the main contribution changing the behavior of the total free energies corresponding to the different solubilizates is the A block-solubilizate mixing free energy (A, Dil). As the interaction parameter χ_{AJ} decreases from hexane to cyclohexane to benzene, the favorable (negative) mixing free energy progressively leads to higher volume fraction of the solubilizate and a structural change from sphere to cylinder to lamella.

A comprehensive summary of the aggregate morphologies predicted for various Pluronic® block copolymers are summarized in Fig. 2. The equilibrium aggregate structures formed of various block copolymers in the absence of any solubilizate and in the presence of four hydrocarbons are shown in the figure. In the Pluronic® grids shown, the weight fraction of PEO increases as one moves to the right and the molecular weight of the PPO block increases as one goes down. Therefore, the molecules in the left section of the grid are more hydrophobic while those on the right section are more hydrophilic. In the absence of any solubilizate, Pluronics® in the 20 series (L62, L72, L92, L122) form lamellar aggregates, Pluronics® in the 30 series form either lamellae

NO SOLUBILIZATE

L62	L63	L64	P65		F68
L72			P75	F77	
		P84	P85	F87	F88
L92					F98
	P103	P104	P105		F108
L122	P123			F127	

HEXANE

L62	L63	L64	P65		F68
L72			P75	F77	
		P84	P85	F87	F88
L92					F98
	P103	P104	P105		F108
L122	P123			F127	

CYCLOHEXANE

L62	L63	L64	P65		F68
L72			P75	F77	
		P84	P85	F87	F88
L92					F98
	P103	P104	P105		F108
L122	P123			F127	

TOLUENE

L62	L63	L64	P65		F68
L72			P75	F77	
		P84	P85	F87	F88
L92					F98
	P103	P104	P105		F108
L122	P123			F127	

BENZENE

L62	L63	L64	P65		F68
L72			P75	F77	
		P84	P85	F87	F88
L92					F98
	P103	P104	P105		F108
L122	P123			F127	

Fig. 2. Equilibrium aggregate morphologies generated by various Pluronic® block copolymers in the absence of any solubilizate and in the presence of hexane, cyclohexane, toluene and benzene as the solubilizates. The equilibrium structures are those that are predicted to occur in the limit of saturation solubilization of the hydrocarbons. The horizontal lines denote lamellar aggregates, the honeycomb represents cylindrical aggregates and the shaded areas refer to spherical aggregates.

(L63) or cylinders (P103, P123) while Pluronics® containing 40 wt% or more of PEO form spherical aggregates. The solubilization of hexane does not lead to any aggregate shape transitions. However, when the solubilizate is cyclohexane, a cylinder to

lamella transition is predicted for P103 and P123 while a sphere to cylinder transition is suggested for L64 and P84. When toluene is the solubilizate, the sphere to cylinder transition is extended to P104. Finally, for benzene as the solubilizate, the cylindrical aggregates of P103 and P123 as well as the spherical aggregates of L64, P84 and P104 all are predicted to undergo a transition to lamellar aggregates. All the predicted results on this figure correspond to the solubilization limit when the aqueous solution is saturated with the solubilizate. Therefore, it is evident that by choosing an appropriate type of solubilizate and the amount of solubilization, one can induce a desired type of structural transition in the Plutronic® block copolymer system..

4. Concluding remarks

The quantitative prediction of aggregate characteristics discussed in this paper are influenced by the simplifying assumptions that have been made in constructing the model. Firstly, the model presented here assumes a sharp interface and does not allow the penetration of water or of the hydrophilic block into the hydrophobic core. It is of interest to relax this assumption and examine how the model predictions will be modified for the case of a diffuse interface. Secondly, for solubilizates such as benzene which are also good solvents for PEO, there is the possibility that in addition to the solubilizate being present in the micellar core, it could also be present in the micellar shell. The model presented here does not describe such a situation. The presence of any solubilizate in the micellar shell can alter the predicted micellar dimensions and the solubilization capacity. Third, only approximate estimates for the interfacial tension σ_{agg} characteristic of the hydrophobic core-hydrophilic corona interface are employed in the present calculations. To obtain improved estimates of σ_{agg}, future developments in the treatment of a constrained interface between two solutions are necessary. Fourth, the PEO–water interactions in corona region are described using the Flory model and taking a constant value for the PEO–water interaction parameter χ_{BW}. However, it is well known that accurate representation of the liquid–liquid phase equilibrium behavior of PEO–water systems require a χ_{BW} that is dependent on temperature, composition of the solution and the molecular weight of the polymer, if the Flory equation is used. Therefore, a fundamental thermodynamic theory of PEO–water system would be necessary to more fully account for the interactions in the corona region. All of the above features would lead to changes in the magnitude as well as size dependence of the free energy and thus have an impact on all the predicted structural features of aggregates including the extent of solubilization. Further, the PPO–water interactions are also represented in the model using a constant vale for χ_{AW}, obtained from vapor–liquid equilibrium studies. Small changes in the estimate for this interaction parameter will significantly affect the magnitude of the free energy of solubilization, but not its dependence on the aggregate size and the composition. Consequently, the calculated CMC can be considerably modified by changes in χ_{AW}, whereas all the predicted structural features of aggregates would remain unaffected. Considering the experimental studies, all the results presented in this work have been obtained on commercial samples of Pluronic® block copolymers. These may contain impurities such as homopolymers PEO, PPO, and block copolymers of differing molecular weights and compositions which can potentially affect the aggregation and solubilization behaviors. The corresponding predictive calculations, however, have been performed for pure block copolymers having the molecular weight and composition specified for the commercial products.

We have enumerated above some possible reasons for a conflict between theoretical predictions and experiments and also the limitations of the predictive calculations. Having said that, one can still recognize the main advantage of the present theory in that it allows completely a priori prediction of all the microstructural features of micelles containing solubilizates with only minor computational efforts. Another advantage of the theory is that all free energy contributions are given as explicit analytical functions directly linked to

physicochemical changes accompanying micellization and solubilization, and involving only molecular constants and geometrical variables. Since our attempt has been to make predictions using well defined models and molecular constants rather than to fit empirically the experimental data, we can take advantage of any observed contradictions between the predictions and the experiments to improve or modify the free energy expressions and to improve the estimates for the molecular constants. Further, new physical effects mentioned in the earlier paragraph (such as the location of the solubilizate partly in the corona region) which are not included in the present model can also be explored. However, to justify meaningful future developments in the theory of solubilization, it is essential to have more detailed measurements of various microstructural characteristics of micelles than are presently available. For example, if we have the core and corona dimensions, aggregate shapes and the amount solubilized for at least a few block copolymers, we can test and improve the model by stipulating that all of the available structural features should be predicted self-consistently by the theory. It is hoped that such experimental studies would be undertaken in the future and facilitate a critical evaluation and development of the theory of solubilization.

Although the focus of this paper has been on hydrophobic low molecular weight solubilizates, the Pluronic® block copolymer has also been used to solubilize both hydrophobic and hydrophilic enzymes [28] and a variety of polar organic molecules like ketone, esters, alcohols and aldehydes [29]. A theoretical treatment of the solubilization behavior of such substances remains to be developed. We had mentioned earlier that both PEO and PPO blocks may serve as loci of solubilization in the case of the hydrophobic aromatic solubilizates. Such a situation is likely to be relevant also for the solubilization of proteins and the polar organic solubilizates. Further experimental studies of solubilization of these types of solutes by Pluronics® will be useful in the development of theories of solubilization governing such solutes. More importantly, such solubilization studies can be useful for developing practical applications for aqueous block copolymer solutions such as for bioproducts recovery that is currently being developed in our laboratory.

References

[1] Z. Tuzar, P. Kratochvil, Surf. Colloid Sci. 15 (1993) 1.
[2] P. Alexandridis, T.A. Hatton, Colloids Surf. A Physicochem. Eng. Asp. 96 (1995) 1.
[3] (a) R. Nagarajan, Curr. Opin. Colloid Interf. Sci. 1 (1996) 391. (b) R. Nagarajan, Curr. Opin. Colloid Interf. Sci. 2 (1997) 282.
[4] R. Nagarajan, M. Barry, E. Ruckenstein, Langmuir 1 (1986) 210.
[5] R. Nagarajan, K. Ganesh, Macromolecules 22 (1989) 4312.
[6] R. Nagarajan, K. Ganesh, J. Colloid Interf. Sci. 184 (1996) 489.
[7] A.N. Semenov, Sov. Phys. JETP 61 (1985) 733.
[8] R. Nagarajan, E. Ruckenstein, Langmuir 7 (1991) 2934.
[9] R. Nagarajan, K. Ganesh, J. Chem. Phys. 98 (1993) 7440.
[10] (a) P.N. Hurter, J.M.H.M. Scheutjens, T.A. Hatton, Macromolecules 26 (1993) 5030. (b) P.N. Hurter, J.M.H.M. Scheutjens, T.A. Hatton, Macromolecules 26 (1993) 5592.
[11] A.V. Kabanov, I.R. Nazarova, I.V. Astafieva, E.V. Batrakova, V. Yu. Alakhov, A.A. Yaroslavov, V.A. Kabanov, Macromolecules 28 (1995) 2303.
[12] F. Gadelle, W.J. Koros, R.S. Schechter, Macromolecules 28 (1995) 4883.
[13] G. Wu, B. Chu, D.K. Schneider, J. Phys. Chem. 99 (1995) 5094.
[14] M. Tian, E. Arca, Z. Tuzar, S.E. Webber, P. Munk, J. Polym. Sci. B Polym. Phys. 33 (1995) 1713.
[15] R. Nagarajan, Colloids Surf. A Physicochem. Eng. Asp. 71 (1993) 39.
[16] R. Nagarajan, in: S.E. Webber, P. Munk, Z. Tuzar (Eds.), Solvents and Self-Organization of Polymers. In: NATO ASI Series, vol. 327, Kluwer Academic, Dordrecht, 1996, p. 121.
[17] P.G. de Gennes, Scaling Concepts in Polymer Physics, Cornell University, Ithaca, 1979.
[18] P.J. Flory, Principles of Polymer Chemistry, Cornell University, Ithaca, 1962.
[19] W.H. Stockmayer, J. Polym. Sci. 15 (1955) 595.
[20] K.S. Siow, D. Patterson, J. Phys. Chem. 77 (1973) 356.
[21] H. Jacobsen, W.H. Stockmayer, J. Chem. Phys. 18 (1950) 1600.
[22] Y.C. Bae, J.J. Shim, D.S. Soane, J.M. Prausnitz, J. Appl. Polym. Sci. 47 (1993) 1193.
[23] K. Schillen, W. Brown, R.M. Johnsen, Macromolecules 27 (1994) 4825.

[24] K. Mortensen, J.S. Pedersen, Macromolecules 26 (1993) 805.
[25] J. Rassing, D. Attwood, Int. J. Pharm. 24 (1983) 47.
[26] G. Wanka, H. Hoffmann, W. Ulbricht, Colloid Polym. Sci. 268 (1990) 101.
[27] Z. Zhou, B. Chu, Macromolecules 20 (1987) 3089. (b) Z. Zhou, B. Chu, Macromolecules 21(1988) 2133.
[28] A. Gupte, R. Nagarajan, A. Kilara, Biotechnol. Prog. 7 (1991) 348.
[29] S.A. Slocum, A. Kilara, R. Nagarajan, in: G. Charalambous (Ed.), Flavors and Off-Flavors, Elsevier Science, Amsterdam, 1990, p. 233.